

# The Distributions of Tau Short and Long Isoforms Fused with EGFP in Cultured Cells

Kosaka Satoru, Takuma Hiroshi, Tomiyama Takami, Mori Hiroshi

<b>Citation</b>	Osaka City Medical Journal. 50(1); 19-27
<b>Issue Date</b>	2004-06
<b>Type</b>	Journal Article
<b>Textversion</b>	Publisher
<b>Right</b>	© Osaka City Medical Association. <a href="https://osakashi-igakukai.com/">https://osakashi-igakukai.com/</a> .

Placed on: Osaka City University Repository

# The Distributions of Tau Short and Long Isoforms Fused with EGFP in Cultured Cells

SATORU KOSAKA, HIROSHI TAKUMA, TAKAMI TOMIYAMA, and HIROSHI MORI

*Department of Neuroscience, Osaka City University Medical School*

## Abstract

Frontotemporal dementia and parkinsonism linked to chromosome 17 (FTDP-17) are caused by mutations of the *TAU* gene. Many such mutations are located near the splicing site of exon 10 and affect the splicing ratio of 3-repeat/4-repeat tau isoforms (referred to as 3R-tau and 4R-tau) which contain 3 and 4 microtubule-binding domains, respectively. Little is known, however, concerning cellular localization of 3R-tau and 4R-tau. We examined the subcellular localization of tau isoforms in IMR-32 cells under differentiated conditions using the fusion proteins of tau isoforms probed with fluorescent protein (EGFP). 3R-tau was observed in spotty and rarely linear distributions while 4R-tau was observed in linear and sometimes spotty distributions. Together with findings of phase-contrast microscopy of cultured cells, these results indicated that 3R- and 4R-tau were predominantly localized at growth tips/branching points and along neurite processes, respectively. Due to their different localizations, balanced expression of 3R- and 4R-tau may coordinate plastic morphogenesis and stabilization of neurite processes.

Key Words: Tau isoform; IMR-32; Subcellular distribution; EGFP-fused protein

## Introduction

Tau is a phosphoprotein mainly present in neuronal cells that is associated with microtubule structures. Tau is known to promote microtubule assembly as a cytoplasmic binding protein. Beside this fundamental function, Tau has been of great interest because of its cytoplasmic inclusion in neuronal and glial cells in brains of individuals with dementia. Tau inclusions, such as neurofibrillary tangles (NFTs) and Pick bodies, are pathological hallmarks of some types of neurodegenerative disorders referred to as 'tauopathies', including Alzheimer's disease (AD). To study the molecular mechanism of such diseases based on chemical structure, tau has been extensively studied, resulting in the finding of structural features of the projection domain in the amino half region and repeat domain in the carboxyl half region responsible for its principal function. Tau comprises six isoforms in adult human brain with 29 or 58 amino-acid inserts near the amino terminus and three or four tandem repeat domains of 31 or 32 amino-acids in the

---

Received October 22, 2003; accepted November 25, 2003.

Correspondence to: Dr. Mori,

Department of Neuroscience, Osaka City University, Graduate School of Medicine,

1-4-3 Asahimachi, Abeno-ku, Osaka 545-8585, Japan

Tel: +81-6-6645-3921; Fax: +81-6-6645-3922

E-mail: mori@med.osaka-cu.ac.jp

carboxyl half<sup>1)</sup>, which are spliced variants of exons 2, 3 and 10 from the single gene on chromosome 17. Notably, expression of exon 10 to encode the second repeat domain is important for producing a difference of three- and four-repeat domains (referred to as 3R- or 4R-tau, respectively) because repeat domains are involved in its promoting activity of microtubule polymerization.

It has been shown that NFTs contain all six tau isoforms in AD brain<sup>2)</sup>, and that recombinant tau isoforms with three repeats form paired helical-like filaments *in vitro*, whereas tau isoforms with four repeats yield straight filaments<sup>3)</sup>. Because the *TAU* gene was identified as the causal gene for frontotemporal dementia and parkinsonism linked to chromosome 17 (FTDP-17), tau was shown to play a significant role in dementia<sup>4,5)</sup>. Among various *TAU* gene mutations reported, some missense mutations occurring in the microtubule-binding domains were able to explain the potent mechanism in FTDP-17 by which neuronal microtubules lost cytoskeletal and transport function due to decreased promoting activities of microtubule polymerization of tau<sup>6-8)</sup>. On the other hand, the intronic or missense mutations near the splicing site of exon 10 are known to be more common in FTDP-17<sup>9)</sup> and to alter the splicing ratio of 3R- and 4R-tau. Little is known concerning the significance of 3R-tau and 4R-tau isoforms except the *in vitro* promoting activity of microtubule polymerization and pathogenesis. Developmental change of tau isoforms was observed at the gene expression level in rat brain<sup>10)</sup>. This change in tau isoform is thought to be related to neural plasticity<sup>11)</sup>. Here we examined the subcellular distribution of 3R- and 4R-tau probed with fluorescent protein in differentiated IMR-32 neuroblastoma cells and provide further evidence for tau-isoform-specific functions.

## Methods

### **DNA constructs**

All of the tau isoform cDNA constructs used here were prepared from human tau cDNA cloned previously<sup>12)</sup>. The tau isoforms used here were 0N3R, which exhibits the tau isoform with no amino-terminal insert and three-repeat, and 0N4R, which exhibits the tau isoform with had no amino-terminal insert and four-repeat. DNA constructs encoded 352 and 381 amino acids, respectively (numbered according to Goedert et al<sup>2)</sup>). Each tau isoform was amplified by PCR using XhoI and EcoRI linker primers (5'-ATATAACTCGAGATGGCTGAGCCCCGCCAGG-3' and 5'-CGATAAGAATTCTCACAAACCCTGCTTGCCAG-3', respectively) for directional restriction site cloning into the pEGFP-C3 vector (Clontech, Palo Alto, CA) as shown in Figure 1. All constructs were verified by sequencing.

### **Cell culture and transfection**

IMR-32 neuroblastoma cells were maintained in half-mixed medium of low-glucose Dulbecco's Modified Eagle's Medium (DMEM)/RPMI Medium 1640 (Gibco BRL, Grand Island, NY) supplemented with 5% fetal bovine serum. For imaging study, the IMR-32 cells ( $5 \times 10^3$ ) were seeded onto poly-D lysine-coated 30 mm glass bottom dishes and incubated for 24 h. One  $\mu$ g of each tau isoform/pEGFP-C3 DNA construct and control vector (pEGFP-C3) was introduced into IMR-32 cells transiently by using LIPOFECTAMINE Reagent (Life Technologies, Gaithersburg, MD) according to the manufacture's recommendation. After transfection, the cells were incubated in differentiated condition as half-mixed medium of low-glucose DMEM/RPMI Medium 1640 supplemented with 5  $\mu$ M of retinoic acid for 72 h. For blotting study, the IMR-32 cells

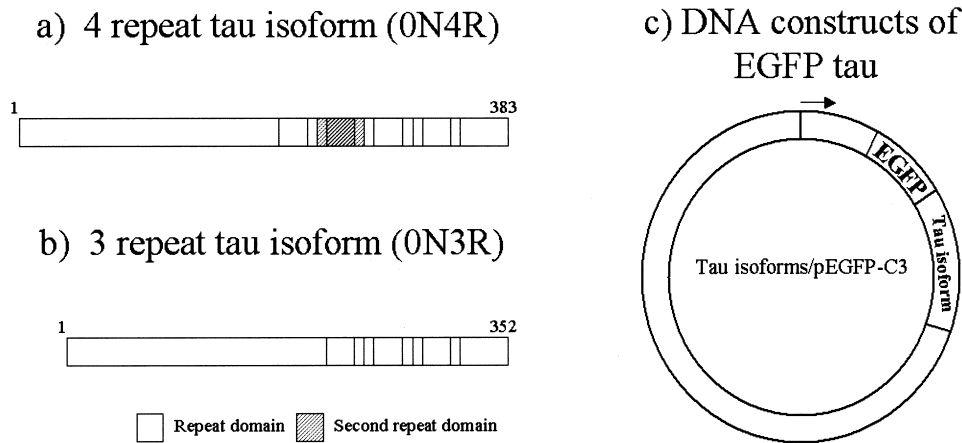


**Figure 1.** Two tau proteins and the illustration of tau construct used here. (a and b) Four repeat tau isoform referred to as 0N4R contains four functional domains (shadow) while three repeat tau isoforms referred to as 0N3R contains three functional domains that lacks the second repeat one. The second repeat domain is encoded by exon10 and is the important exon whose abnormal expression causes FTDP-17. (c) Either of two tau isoforms is ligated with EGFP in frame to produce a fusion protein. The arrow indicates the transcription direction of the of tau-EGFP fusion gene in the vector.

were seeded onto poly-D lysine-coated 100 mm dishes and incubated to achieve 70% confluency one day prior to transfection. Four  $\mu\text{g}$  of each DNA construct was used for transfection. Transfection and incubation were performed as the protocol done in imaging study.

#### ***Permeabilization of cell membranes and drug treatment***

To examine the cytoskeletal association of EGFP-tau, transfected cells were gently treated with 0.1% Triton X-100 for 30 sec at 37  $^{\circ}\text{C}$  to disrupt cell membranes by making pores to enable soluble or unbound cytoplasmic proteins permeable and washed away.

#### ***Sodium dodecyl sulfate (SDS)-polyacrylamide gel electrophoresis and immunoblotting***

The cells in culture dishes were scraped into 50  $\mu\text{L}$  of Tris-buffered saline (TBS; 50 mM Tris-HCl and 150 mM NaCl) adjusted at pH 8.5 and homogenized by sonication. The homogenates were centrifuged at 15000g for 10 min. To precisely compare the molecular weights of tau fusion proteins and to delete apparent molecular changes due to their modification of phosphorylation in cells<sup>13</sup>, the resultant supernatants were dephosphorylated by incubating with 400 units of alkaline phosphatase (Sigma, St. Louis, MO) and 0.1 mM EDTA at 67  $^{\circ}\text{C}$  for 3 h. SDS sample buffer was added to the dephosphorylated samples to obtain a final concentration of 2% SDS, 80 mM Tris pH 6.8, 10% glycerol and 5%  $\beta$ -mercaptoethanol. Samples corresponding to one-fifth of the collected cells were applied to 10% polyacrylamide gels for electrophoresis followed by blotting onto polyvinylidene difluoride (PVDF) membrane. The membrane was blocked with 3% milk and 1% bovine serum albumin solution in TBS adjusted at pH 7.6, incubated with the primary anti-EGFP monoclonal mouse antibody JL-8 (Clontech) diluted to 1:2000 for 3 h at room temperature, and then incubated with the secondary horseradish peroxidase-conjugated goat anti-mouse antibody (BIO-RAD, Hercules, CA) diluted to 1:5000 for 1 h at room temperature. An ECL+ chemiluminescence detection kit ECL+ (Amersham Biosciences, Piscataway, NJ) was used for visualization. Blotting image scanning was performed with the LAS-1000 Bio-Imaging Analyzer System (Fuji film, Tokyo, Japan).

### Confocal analysis

The transfected living cells were observed by confocal laser microscopy LSM510 (Carl Zeiss, Oberkochen, Germany). Green spots at the tips of neurites and branches were counted as spotty distribution, and green lines along the neurites as a linear distribution. If no transfected cells were observed in the selected field, the field was omitted. We used the L/S ratio, in which L and S represent linear (aspect ratio of fluorescent area more than 2) and spotty (aspect ratio of fluorescent area 1 to less than 2) distributions, respectively. The L and S values were summed for ten scanning fields obtained in one transfection experiment. To enable statistical testing of the L/S ratio, the experiments were repeated ten times to obtain 100 images for each tau isoform construct. One-way factorial ANOVA was performed to determine whether differences were significant, and the Tukey-Kramer test was then further employed to determine the significance that was set at  $p < 0.01$ .

## Results

### Tau expression

EGFP-tau fusion proteins were expressed in human neuroblastoma IMR-32 cells. With anti-EGFP antibody (JL-8) we observed a single band with a molecular weight of 23 kDa that represented EGFP expressed from the mock vector, while we observed several bands in the high-molecular-weight range representing EGFP-tau isoform-fused proteins (3R-tau and 4R-tau) whose molecular weights were estimated to be 71 and 75 kDa, respectively, that were almost equivalent to the simple summation of the two molecular weights of tau protein<sup>14</sup> and EGFP (Fig. 2). Free EGFP or degradation products were virtually absent in cells transfected with EGFP-tau fused proteins. Thus, constructs for encoding EGFP-tau fusion proteins were successfully prepared as reliable probes for the following experiments.

### Subcellular distribution of Tau isoforms

To analyze the subcellular localization of EGFP-tau fusion proteins, IMR-32 cells were induced to differentiate by retinoic acid. As shown in Figure 3, a considerable number of cells exhibited well-developed branching and unbranching neurites, which are morphological hallmarks of neuronal processes. When we used 0N3R tau, which had no amino-insert and

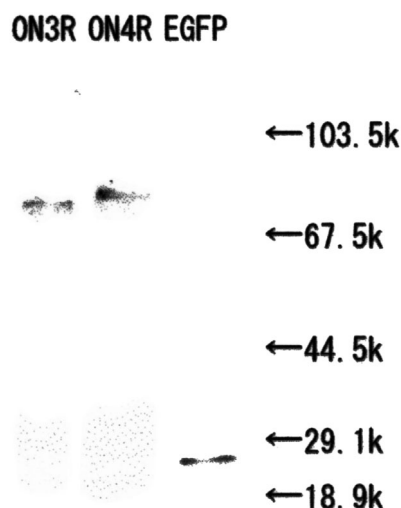


**Figure 2.** Gene expression of EGFP-tau fusion protein in IMR-32 cells. IMR-32 cells were transfected with EGFP-tau isoforms and the resultant cell lysates were examined with anti-EGFP antibody. A single band was stepwise detected in each lane. In the right lane, the control sample of cell lysates transfected with EGFP-C3 vector yield a single band representing EGFP-C3 with a molecular weight of 23 kDa. The two left lanes represent the fusion proteins of EGFP and each tau isoform (0N3R and 0N4R). Their molecular weights were estimated to be 71 and 75 kDa, respectively, to correspond with summation of the respective molecular weights of tau proteins (48 kDa and 52 kDa, respectively) and EGFP (23 kDa). Notably, there were intact and full-sized fused proteins but little aggregation and few degradations of fused proteins in cells.



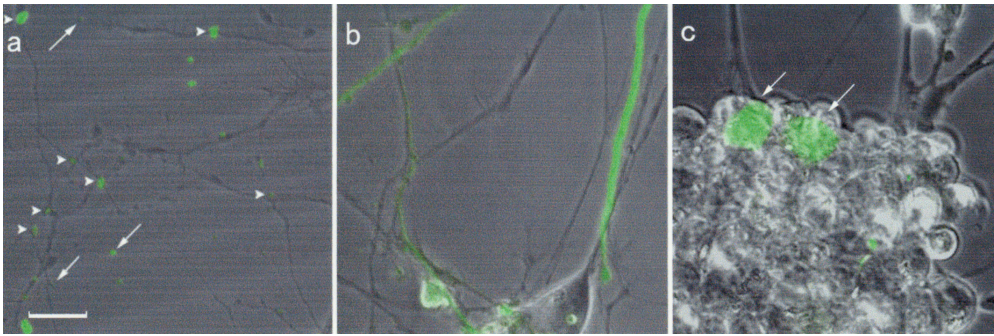


**Figure 3.** Fluorescent images of transfected living IMR-32 cells. IMR-32 cells were transfected with EGFP-tau isoforms and the resultant transfected living IMR-32 cells were observed by confocal microscopy. (a) In EGFP-tau (0N3R), spotty distribution of fluorescent protein was observed at branching points (arrowhead) and growth tips (arrow) when was introduced. (b) In EGFP-tau (0N4R), linear distribution along neurites was observed. (c) In mock experiment with EGFP-C3 vector alone, somal distribution was solely fluorescent. Scale bar: 20  $\mu\text{m}$ .

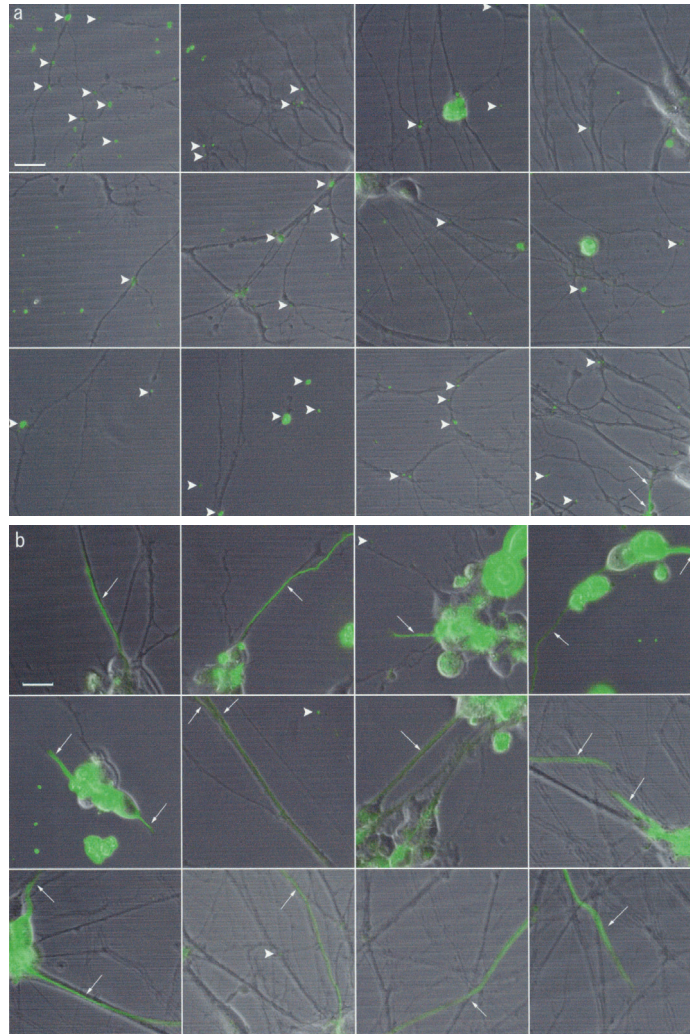


**Figure 4.** Confocal laser microscopic views of EGFP-tau isoforms (0N3R and 0N4R). (a) Various fluorescent images for an EGFP-tau isoform (0N3R). Most images revealed a spotty distribution. Some, although very few, linear distributions were also observed (arrows). (b) Various fluorescent images for another EGFP-tau isoform (0N4R). Most images revealed the linear distribution. Linear and some spotty distributions were indicated by arrow and arrowheads, respectively. Scale bars: 20  $\mu\text{m}$ .

three-repeat domains, for transfection, fluorescent proteins were mostly distributed as spots on the branches (arrowhead) and the growth cones (arrow) of the neurites in addition to the perikarya (Fig. 3a). In contrast, when we used 0N4R tau, which had no amino-insert and four repeat domains, we observed distinct fluorescent images. Fluorescent proteins were mostly distributed linearly along the neurites in addition to the perikarya (Fig. 3b). With use of the control vector alone without any tau sequence, the fluorescent EGFP were observed mostly in perikarya with only very small amounts in neurite processes (arrow in Fig. 3c).

These differences in distribution between 3R-tau and 4R-tau isoforms were reproducibly observed. Figure 4 a and b show various fluorescence images for both EGFP-3R and EGFP-4R isoforms, respectively. As shown in Figure 4a, EGFP-3R-tau isoform (0N3R) exhibited a predominantly spotty distribution and very few linear distributions. On the other hand, EGFP-4R-tau isoform (0N4R) exhibited principally linear distributions and small numbers of spotty distributions (arrowheads, Fig. 4b). Thus, these differences between these two tau isoforms in subcellular distribution were highly characteristic but not absolutely exclusive. Both 3R- and 4R-tau isoforms exhibited perikaryal distribution, although 4R-tau isoform seemed to be more prominent there (Fig. 3, b and c).

#### ***EGFP-tau isoform fusion proteins are associated with cellular microtubules***

It remained unclear whether EGFP-tau fusion proteins were associated with cellular microtubules. Although EGFP-tau fusion proteins were found in living intact neuronal cells (Figs. 3 and 4), we could not rule out the possibility that EGFP-tau fusion proteins were present in a free form in the cytoplasm rather than in a bound form associated with microtubules. As shown in Figure 5, considerable amounts of fluorescence associated with EGFP-tau fusion proteins remained after detergent treatment with 0.1% Triton X-100 to permeabilize cell membranes. Careful observation revealed little change in fluorescent images of spotty and linear distributions in cells transfected with EGFP-tau isoforms (0N3R or 0N4R) (Fig. 5), indicating that both 3R- and 4R-tau were tightly associated with cytoskeletal microtubule structures and not in free or soluble form, as described before<sup>15-17</sup>. We therefore concluded that both EGFP-3R- and 4R-tau fusion proteins were associated with cellular microtubules.

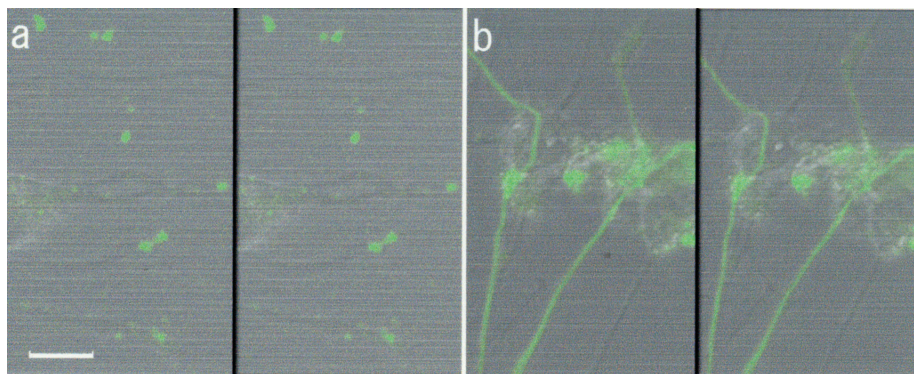


**Figure 5.** EGFP-tau is associated with cellular microtubules. (a) Fluorescent images of EGFP-tau isoforms (0N3R and 0N4R) were retained on the Triton X-100 treatment for 30 sec at 37 °C; the left and right windows in each column represent observations before and after the Triton X-100 treatment of cells with (a) EGFP-tau (0N3R), (b) EGFP-tau (0N4R), respectively. These results suggested that both 3R- and 4R-tau but not free EGFP were associated with cellular microtubules. Scale bar: 20  $\mu$ m.

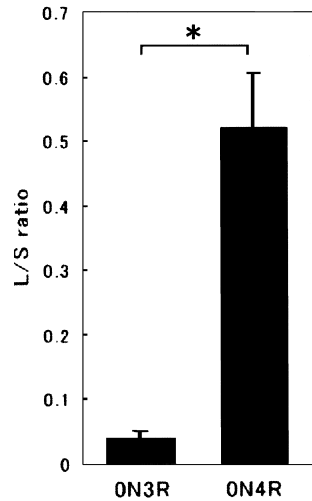


**Figure 6.** Static analysis of distributions of EGFP-3R-tau isoform and EGFP-4R-tau isoform. Significant differences were observed between 0N3R and 0N4R (Tukey-Kramer test (\*);  $p < 0.01$ ). 4R-tau featured a significantly larger L/S ratio than 3R-tau. The error bars shows the SD of the samples ( $n = 10$ ).

We quantitatively evaluated the differences in distribution among EGFP-tau isoforms as shown in Figures 3 and 4. We counted the numbers of spotty and linear distributions of each tau isoform in a hundred fields in total for ten transfection studies (ten fields for each transfection). The L/S ratios for 0N3R and 0N4R tau were  $0.039 \pm 0.006$  (mean  $\pm$  SD),  $0.520 \pm 0.111$ , respectively. Significant differences were observed between 0N3R and 0N4R ( $n = 10$ ,  $p < 0.01$ , Tukey-Kramer test) as clearly demonstrated in Figure 6.

## Discussion

We showed here distinct distributions of 3R- and 4R-tau isoforms fused with EGFP in spotty and linear configurations, respectively. 3R-tau was preferentially localized in the neurite growth tips and branching regions, where neurites are thought to grow coupled with dynamic microtubules<sup>11,18</sup>. On the other hand, 4R-tau was preferentially localized in the linear neurite stems and processes where microtubules are thought to be in relatively stable condition compared with that in neurite growth tips or branching regions. Little evidence accumulated concerning the stability of microtubules at branching points of neurites. On a view of tau isoforms distribution, the present study suggests that branching points of neurites are in a similar microtubule condition to neurite tips or growth cones.

The EGFP-tau fusion protein was initially shown to be a useful probe in previous studies<sup>17,19</sup> in which its subcellular distribution was found to be indistinguishable from that of tau without EGFP. A recent study using fluorescently-tagged tau successfully revealed disturbance of the axonal flow followed by neuronal degeneration<sup>20</sup>. It remains, however, uncertain whether 3R-tau has an effect similar to that of 4R-tau reported there. We designed two fusion proteins with 3-repeat- or 4-repeat-domains according to these references and confirmed fusion proteins at the protein expression and subcellular distribution (Fig. 1). Exogenous EGFP-tau fusion protein was supposed to intermingle and work together with endogenous tau in a somewhat competitive fashion. Since EGFP-tau fusion proteins contained an extra-sequence derived from EGFP, we could not exclude the possibility that the fusion proteins were less potent in their promoting activities of microtubule polymerization than non-fused endogenous tau proteins. Despite this possibility, it is worthy to use EGFP-tau fusion proteins and to discuss their subcellular distributions and functions, at least on the basis of comparison as shown here. As repeatedly



disputed, the tubulin-binding ability of 3R-tau is claimed to be less than that of 4R-tau<sup>14,21-23</sup>). Our finding that repeat number affects the distribution of EGFP-tau fusion protein may be partly explained by differences among tau isoforms in tubulin binding abilities. It is very likely that the present difference between 3R- and 4R-tau isoforms in subcellular distribution can be explained by the difference in their polymerization velocities, as previously reported<sup>22</sup>).

It is well established that repeat domains play a fundamental role in promoting of polymerization reaction in an assembly-disassembly equilibrium of microtubules. On the other hand, N-inserts are less characterized. Although their involvement in modification of the function of repeat domains were reported, it is still unclear whether N-inserts affect the microtubule-binding ability of tau<sup>14,22,23</sup>).

Most of the FTDP-17 mutations affecting exon 10 splicing have had only an increasing effect on the ratio of 4R/3R-tau expression<sup>4,24,25</sup>) and no effect on the tubulin-binding ability of tau. Only two mutations, intronic G+29A mutation and  $\Delta$ 280K mutation, have been found to decrease the ratio of 4R/3R-tau expression and have remarkably decreased tubulin-binding ability followed by neural degeneration<sup>26-28</sup>). Pick disease exhibits a similar change. In contrast, most cases of FTDP-17, the ratio of 4R/3R-tau expression was increased. In other words, either upregulation or downregulation causes FTDP-17, suggesting that balanced expression of 4R/3R-tau must occur at least in human brain without dementia.

In human brain, 3R-tau is mainly expressed in infants, and 4R-tau expression increases with development and maturation. Taken these observations into consideration, 3R-tau isoforms are thought to play essential roles in growing or developing plastic neurons rather than in developmentally established or stable neurons. The present findings suggest that 3R-tau may be required in balanced ratio in axonal branching and tip for normal coordination with 4R-tau to be associated with axonal microtubules. We speculate too much or too little axonal outgrowth compared with that required for axonal maintenance is the cause of types of neuronal chaos such as that in dementia. Thus, unbalanced expression of 3R- and 4R-tau isoforms could explain the etiology of FTDP-17 as due to not only an excess 4R-tau function but also a loss of 3R-tau-specific function such as neural outgrowth and plasticity and the resultant failure of dynamic turnover of cellular microtubules.

### **Acknowledgement**

Supported in part by a grant-in-aid for Scientific Research on Priority Areas (C)-Advanced Brain Science Project- from the Ministry of Education, Culture, Sports, Science and Technology, Japan (to HM). This study was also supported by grants-in-aid from Uehara Memorial Foundation.

### **References**

1. Goedert M, Spillantini MG, Jakes R, Rutherford D, Crowther RA. Multiple isoforms of human microtubule-associated protein tau: sequences and localization in neurofibrillary tangles of Alzheimer's disease. *Neuron* 1989;3:519-526.
2. Goedert M, Spillantini MG, Cairns NJ, Crowther RA. Tau proteins of Alzheimer paired helical filaments: abnormal phosphorylation of all six brain isoforms. *Neuron* 1992;8:159-168.
3. Goedert M, Jakes R, Spillantini MG, Hasegawa M, Smith MJ, Crowther RA. Assembly of microtubule-associated protein tau into Alzheimer-like filaments induced by sulphated glycosaminoglycans. *Nature* 1996;383:550-553.

4. Hutton M, Lendon CL, Rizzu P, Baker M, Froelich S, Houlden H, et al. Association of missense and 5'-splice-site mutations in tau with the inherited dementia FTDP-17. *Nature* 1998;18:702-705.
5. Poorkaj P, Bird TD, Wijsman E, Nemens E, Garruto RM, Anderson L, et al. Tau is a candidate gene for chromosome 17 frontotemporal dementia. *Ann Neurol* 1998;43:815-825.
6. Hasegawa M, Smith MJ, Goedert M. Tau proteins with FTDP-17 mutations have a reduced ability to promote microtubule assembly. *FEBS Lett* 1998;437:207-210.
7. Hong M, Zhukareva V, Vogelsberg-Ragaglia V, Wszolek Z, Reed L, Miller BI, et al. Mutation-specific functional impairments in distinct tau isoforms of hereditary FTDP-17. *Science* 1998;282:1914-1917.
8. Trinczek B, Ebnet A, Mandelkow EM, Mandelkow E. Tau regulates the attachment/detachment but not the speed of motors in microtubule-dependent transport of single vesicles and organelles. *J Cell Sci* 1999;112:2355-2367.
9. Morris HR, Khan MN, Janssen JC, Brown JM, Perez-Tur J, Baker M, et al. The genetic and pathological classification of familial frontotemporal dementia. *Arch Neurol-Chicago* 2001;58:1813-1816.
10. Kosik KS, Orecchio LD, Bakalis S, Neve RL. Developmentally regulated expression of specific tau sequences. *Neuron* 1989;2:1389-1397.
11. Goode BL, Feinstein SC. Identification of a novel microtubule binding and assembly domain in the developmentally regulated inter-repeat region of tau. *J Cell Biol* 1994;124:769-782.
12. Mori H, Hamada Y, Kawaguchi M, Honda T, Kondo J, Ihara Y. A distinct form of tau is selectively incorporated into Alzheimer's paired helical filaments. *Biochem Biophys Res Commun* 1989;159:1221-1226.
13. Alonso AD, Zaidi T, Novak M, Barra HS, Grundke-Iqbal I, Iqbal K. Interaction of tau isoforms with Alzheimer's disease abnormally hyperphosphorylated tau and *in vitro* phosphorylation into the disease-like protein. *J Biol Chem* 2001;276:37967-37973.
14. Goedert M, Jakes R. Expression of separate isoforms of human tau protein: correlation with the tau pattern in brain and effects on tubulin polymerization. *EMBO J* 1990;9:4225-4230.
15. Merrick SE, Demoise DC, Lee VM. Site-specific dephosphorylation of tau protein at Ser202/Thr205 in response to microtubule depolymerization in cultured human neurons involves protein phosphatase 2A. *J Biol Chem* 1996;271:5589-5594.
16. Perez M, Lim F, Arrasate M, Avila J. The FTDP-17-linked mutation R406W abolishes the interaction of phosphorylated tau with microtubules. *J Neurochem* 2000;74:2583-2589.
17. Lu M, Kosik KS. Competition for microtubule-binding with dual expression of tau missense and splice isoforms. *Mol Biol Cell* 2001;12:171-184.
18. Bramblett GT, Goedert M, Jakes R, Merrick SE, Trojanowski JQ, Lee VM. Abnormal tau phosphorylation at Ser396 in Alzheimer's disease recapitulates development and contributes to reduced microtubule binding. *Neuron* 1993;10:1089-1099.
19. Nagiec EW, Sampson KE, Abraham I. Mutated tau binds less avidly to microtubules than wildtype tau in living cells. *J Neurosci Res* 2001;63:268-275.
20. Stamer K, Vogel R, Thies E, Mandelkow E, Mandelkow EM. Tau blocks traffic of organelles, neurofilaments, and APP vesicles in neurons and enhances oxidative stress. *J Cell Biol* 2002;156:1051-1063.
21. Lee G, Neve RL, Kosik KS. The microtubule binding domain of tau protein. *Neuron* 1989;2:1615-1624.
22. Gustke N, Trinczek B, Biernat J, Mandelkow EM, Mandelkow E. Domains of tau protein and interactions with microtubules. *Biochemistry-U S A* 1994;33:9511-9522.
23. Goode BL, Chau M, Denis PE, Feinstein SC. Structural and functional differences between 3-repeat and 4-repeat tau isoforms. Implications for normal tau function and the onset of neurodegenerative disease. *J Biol Chem* 2000;275:38182-38189.
24. Murrell JR, Koller D, Foroud T, Goedert M, Spillantini MG, Edenberg HJ, et al. Familial multiple-system tauopathy with presenile dementia is localized to chromosome 17. *Am J Hum Genet* 1997;61:1131-1138.
25. Spillantini MG, Murrell JR, Goedert M, Farlow MR, Klug A, Ghetti B. Mutation in the tau gene in familial multiple system tauopathy with presenile dementia. *Proc Natl Acad Sci USA* 1998;23:7737-7741.
26. Rizzu P, Van Swieten JC, Joosse M, Hasegawa M, Stevens M, Tibben A, et al. High prevalence of mutations in the microtubule-associated protein tau in a population study of frontotemporal dementia in the Netherlands. *Am J Hum Genet* 1999;64:414-421.
27. Barghorn S, Zheng-Fischhofer Q, Ackmann M, Biernat J, von Bergen M, Mandelkow EM, et al. Structure, microtubule interactions, and paired helical filament aggregation by tau mutants of frontotemporal dementias. *Biochemistry-U S A* 2000;26:11714-11721.
28. Stanford PM, Shepherd CE, Halliday GM, Brooks WS, Schofield PW, Brodaty H, et al. Mutations in the tau gene that cause an increase in three repeat tau and frontotemporal dementia. *Brain* 2003;126:814-826.